Spatio-Temporal Recommender for V2X Channels

Maqsood Ahamed Abdul Careem
Department of Electrical and Computer Engineering
University at Albany, SUNY
Albany, NY 12222

Aveek Dutta
Department of Electrical and Computer Engineering
University at Albany, SUNY
Albany, NY 12222

***Abstract*—Recommending channel characteristics for V2X communication has the distinct advantage of pre-conditioning the waveform at the transmitter to *match* the expected fading profile. The difficulty lies in extracting an accurate model for the channel, especially if the underlying variables are uncorrelated, unobserved and immeasurable. Our work implements this prescience by assimilating the Channel State Information (CSI), obtained as a feedback from vehicles, over time and space to adjust the modulation vectors such that the channel impairments are significantly diminished at the receiver, improving the Bit Error Rate (BER) by 96% for higher order modulations. To account for the multivariate, non-stationary V2X channel, a tensor decomposition and completion approach is used to mitigate the effects of sparsity and noise in the CSI measurements. Overall, the system is shown to operate with a prediction accuracy of 10^{-3} MSE even in dense scattering environments over space and time.**

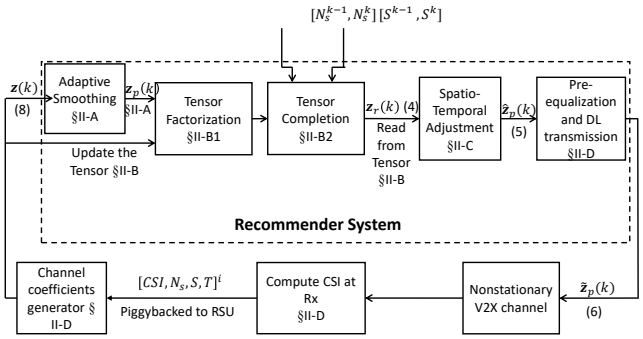

Figure 1: V2X Channel recommender system. The corresponding equations are indicated in parenthesis along with the sections for the description within the text.

I. Introduction

Recommender systems are designed to bridge the gap between the desired and actual behavior of a partially known (or sometimes unknown) process by iteratively tracking certain patterns in the outcomes. In turn, this reduces the ambiguity and uncertainty in the decision making process for the end-user. Wireless communication between a Vehicle (V) to Anything (X), termed as V2X [1], is analogous to such a recommender system, where the receiver can significantly reduce its packet (or bit) error rate, only if the transmitter (Road-Side Unit (RSU) or another vehicle) uses the *recommended* signal parameters based on historically observed channel profiles, obtained as a feedback from the receivers. Intuitively, if the transmitter pre-conditions the waveform with the mathematical inverse of the expected channel, the received signal will likely contain minimal amount of distortion.

This problem is complicated due to unknown and immeasurable relationships among the factors contributing to the fading profile of the channel, that also vary over space and time. Most importantly, the localized scattering from nearby vehicles, road-side features like buildings and vegetation, Doppler spectrum and path-loss, are either stochastic variables or time-variant. Collectively, these properties make the V2X channel statistically non-stationary [2], [3]. Our goal in this work is to rely on measurable parameters like vehicle density (N_s), vehicle location, mapped into quasi-stationary segments (S) [4] and the CSI feedback (CSI) to construct a non-uniformly spaced, non-stationary time series (indexed by time of reception, T). The CSI from the receivers captures a wide variety of channel characteristics across a stretch of road under different scattering environments. Broadband communication using frequency domain modulation such as Orthogonal Frequency Division Multiplexing (OFDM) used in the standards advocated for WAVE [5] also captures the channel profile in frequency domain. Figure 1 shows the channel recommender system for V2X communication. It operates on the quadruplet, $[CSI, N_s, S, T]^i$, obtained from vehicle i.

The first step is to pre-process the CSI using an adaptive filter (e.g., a combination of autoregression (AR) and Kalman filter [6], [7]), to dampen the effects of non-linearities in the estimation process in the receiver and the uplink channel. This is used in the second step to predict the downlink channel profile for any target vehicle in the road, according to its position and the scattering environment. This is accomplished by constructing a third order tensor containing the transitions for number of scatterers, $[N_s^{k-1}, N_s^k]$ and segment number, $[S^{k-1}, S^k]$ from the last observed CSI in time-step k and the corresponding error in the recommended channel. This is described in §II-B,C. After this adjustment, the final step is to pre-condition the waveform, such that the receiver estimates an almost flat fading across all subcarriers (in §II-D). This step eliminates the need for any complex receiver side algorithm [8] and is also compatible with conventional pilot based equalization. As the recommender system evolves with more spatio-temporal CSI, the gap between the recommended and the true channel gets asymptotically small leading to almost two orders of magnitude improvement in the BER for QAM modulations. Experiments in §III explore various trade-offs and performance of the recommender system.

Non-stationary V2X Channel: V2X channels are modeled using the Geometric Stochastic Channel Model (GSCM), which forms the basis of the widely used WINNER channel model [4]. The V2X channel at time k and for the n^{th} OFDM subcarrier, depends on factors like, the number of scatterers at time k, $N_s(k)$, Doppler frequency, the angle of departure (AoD) and angle of arrival (AoA), complex channel gains and path delays for each sub-path. The AoAs and AoDs are functions of the transmitter (RSU or vehicle) location, vehicle (receiver) location, and number of scatterers in each (elliptical) scattering zone that are stochastically distributed [7]. The path delay (and consequently the channel impulse response) collectively depend on these factors. This non-stationarity over space, time and vehicular density affect the reliability and latency of data transmission, which has also been validated by various measurement campaigns [2].

II. Channel Recommendation System

The CSI is a quantized estimate of the downlink channel that can be used to adjust the parameters for future transmissions. However, the high dynamics of the V2X network requires agile scheduling of packets at the RSU for links with different scattering environment and location. Hence, the CSI may become obsolete (without further processing), and the RSU has the added burden of making unique recommendations for every downlink packet. To address this problem we design a recommender system that has four stages as shown in figure 1: *A) Adaptive Smoothing:* Iteratively tracks and smooths the non-stationary noise in the CSI (similar to [7]), *B) Tensor Factorization & Completion:* This step generates channel recommendations to account for the change in the scattering environment and location of vehicles over time. *C) Spatio-Temporal Adjustment:* The output of steps A and B is fused to form the recommended downlink channel profile for the next packet, and *D) Pre-Equalization:* The downlink waveform is pre-equalized using the recommended channel profile, to achieve flat fading at the receiver. In this paper, we focus on step B and step C as above, while adopting steps A and D from the literature [7].

The RSU processes the channel state, received as a quadruplet $[CSI, N_s, S, T]^i$ for each vehicle i, whenever it is available (typically piggy-backed on an acknowledgement packet). It is to be noted that any two CSI are statistically different even if the other values in the quadruplet remain unchanged. The recommender system operates in real-time, requires minimal training and lowers the BER even when the tensor is 99% sparse and contains noisy measurements.

A. Adaptive Smoothing

Adaptive smoothing of non-stationary noise in the CSI can be performed by a combination of autoregression (AR) and Kalman filter. The CSI obtained from the various vehicles are combined using a noisy autoregressive (AR) model (random walk), the weights of which are tracked by a Kalman filter as in [6], [7]. However, this iterative approach results in a lag between the tracked channel and the actual channel, due to one time-step delay in the CSI feedback path as shown in figure 2. Hence, an additional smoothing step (similar to [6]) is employed to mitigate the effect of this lag and any undesired transients in the received CSI. We denote it by $\mathbf{z}_p(k)$ and use it in §II-B and §II-C. Although the smoothing step reduces transients, it is unable to maintain low error vector magnitude (EVM) for higher order modulations. Moreover, a single smoothing filter is unable to simultaneously track the channel statistics over multiple locations and multiple vehicles.

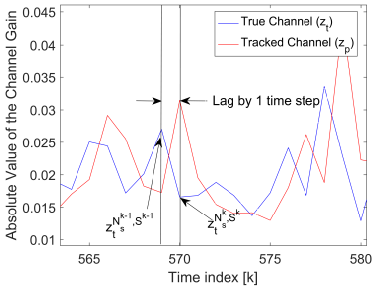

Figure 2: The tracked channel lags the true channel.

B. Tensor Completion & Factorization

It is evident from figure 2, that there is a disconnect between the smoothed channel and the actual channel, which depends on the current scattering environment and location of the receiver. This information is embedded in the CSI, which consequently captures the deviation due to the change in the scatterers and the receiver location. We construct a 3D tensor, shown in figure 3 to capture this property. The purpose of the tensor is to record these deviations and use them to make adjustments (details in §II-C) to the smoothed channel, $\mathbf{z}_p(k)$. The measurement channel, $\mathbf{z}(k)$ derived from the CSI (see §II-D) is recorded in the tensor corresponding to the change in the scatterers (N_s^{k-1}, N_s^k) and segments (S^{k-1}, S^k). This represents a tube containing 100 quantization levels (q). The output of the smoothing filter, $\mathbf{z}_p(k)$ is quantized to the nearest level and the corresponding cell is populated with the measurement channel, $\mathbf{z}(k)$. The cell values are updated as a running average of all measurement channels that are mapped to that particular cell. Therefore, in essence, each cell in the tube contains the historical deviations observed for a given change in N_s and S and the corresponding quantized level for $\mathbf{z}_p(k)$. The quantized levels capture information required to update the recommended channel as in §II-B2 and §II-C.

There are other latent factors that affect these deviations. Moreover, key challenges in this tensor-based procedure are, sparsity (due to the large size of the tensor database detailed in §III and infrequent entries (CSI) that may not be observed over long duration of time), and noisy data in the tensor (due to incomplete filling of cells). These result in missing or corrupt adjustments. Hence, to account for these factors, we introduce tensor factorization & completion (which uses latent factors to account for these missing variables). At each time step k, the channel tensor is updated with the measurement channel, $\mathbf{z}(k)$. This channel tensor is then factorized (§II-B1) into a factor

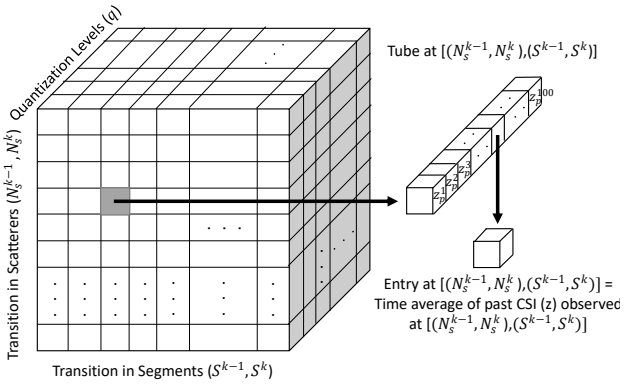

Figure 3: An illustration of tensor $\mathcal{Z}$ and its entries.

model to capture the latent structure of the underlying process under sparse conditions. The tensor is then reconstructed using the factorized model (§II-B2) to extract missing entries. The completed tensor is used to generate recommendations, $\mathbf{z}_r(k)$ which is used to adjust the smoothed channel, $\mathbf{z}_p(k)$ (§II-C) for the location and scattering environment of a target vehicle.

1) Tensor Factorization: Tensor factorization is employed to capture latent structure of the channel tensor by expressing it as the sum of component rank-one tensors [9]. This latent structure is used to reconstruct missing entries in the tensor. Figure 4 shows the tensor factorization of the third order channel tensor. Here, scalars are denoted by lowercase letters (e.g., a), vectors by boldface lowercase letters (e.g., $\mathbf{a}$), matrices by boldface capital letters (e.g., $\mathbf{A}$), higher-order tensors by boldface Euler script letters (e.g., $\mathcal{Z}$). The i^{th} entry of a vector $\mathbf{a}$ is denoted by a_i, element (i,j) of a matrix $\mathbf{A}$ is denoted by a_{ij}, and element (i,j,k) of a third-order tensor $\mathcal{Z}$ is denoted by z_{ijk}. The j^{th} column of a matrix $\mathbf{A}$ is denoted by $\mathbf{a}_j$. The n^{th} element in a sequence is denoted by a superscript in parentheses, e.g., $\mathbf{A}^{(n)}$ denotes the n^{th} matrix in a sequence. Let $\mathcal{Z}$ be the three-way channel tensor of size $I \times J \times K$, and rank R. Then the channel tensor decomposition is defined by factor matrices $\mathbf{A}$, $\mathbf{B}$, and $\mathbf{C}$ of sizes $I \times R$, $J \times R$, and $K \times R$ (defined in figure 4) that minimize the objective function,

$$f_{\mathcal{W}}(A,B,C) = \underbrace{\frac{1}{2}\sum_{i=1}^{I}\sum_{j=1}^{J}\sum_{k=1}^{K}\left\{w_{ijk}\left\{z_{ijk} - \sum_{r=1}^{R} a_{ir}b_{jr}c_{kr}\right\}\right\}^2}_{\text{Error function}} + \underbrace{\frac{\lambda}{2}\sum_{r=1}^{R}\left\{\sum_{i=1}^{I}||a_{ir}||^2 + \sum_{j=1}^{J}||b_{jr}||^2 + \sum_{k=1}^{K}||c_{kr}||^2\right\}}_{\text{Regularization term}} \quad (1)$$

The *error function* is employed to account for CSI noise in the channel tensor (i.e., imperfect data) and the weighted version of the error function is used to address sparsity by ignoring missing data and modeling only the known entries [10]. Consequently, minimizing the above objective function ensures that the recommendations, $\mathbf{z}_r(k)$ accurately represents the discrepancy in channel tracking, even in the case of missing entries. Here, $\mathcal{W}$ denotes a nonnegative weight tensor (representing the sparsity of the channel tensor $\mathcal{Z}$), with entries

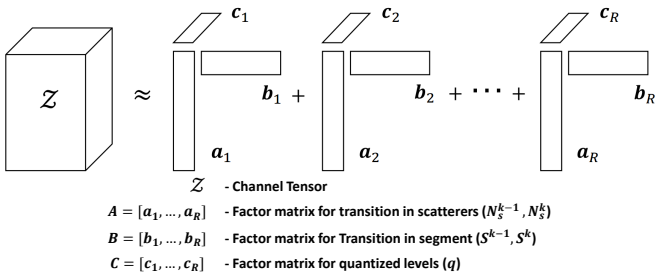

Figure 4: Illustration of tensor factorization for third-order tensors. Here, $\mathbf{A} = [\mathbf{a}_1, ..., \mathbf{a}_R]$, $\mathbf{B} = [\mathbf{b}_1, ..., \mathbf{b}_R]$ and $\mathbf{C} = [\mathbf{c}_1, ..., \mathbf{c}_R]$ represent the factor matrices for the transition in the number of mobile scatterers and transition in segments and quantized levels respectively.

of '1', when z_{ijk} is known and entries of '0', when z_{ijk} is missing, for all $i = 1, \ldots, I, j = 1, \ldots, J, k = 1, \ldots, K$. The *regularization term* penalizes the size of the latent factors and consequently avoids over-fitting the noise in the measurement channel, $\mathbf{z}(k)$ and ensures the generality of the tensor, $\mathcal{Z}$ over space and time. The regularization parameter, λ is a non-negative value that balances the modeling error and the complexity of the latent structure. For convenience the objective function in (1) is expressed as,

$$f_{\mathcal{W}}(\mathbf{A},\mathbf{B},\mathbf{C}) = \frac{1}{2}||\mathcal{Z} - [\![\mathbf{A},\mathbf{B},\mathbf{C}]\!]||^2_{\mathcal{W}} + \frac{\lambda}{2}(||\mathbf{A}||^2 + ||\mathbf{B}||^2 + ||\mathbf{C}||^2) \quad (2)$$

Here $[\![\cdot]\!]$ represents the Kruskal operator shorthand notation [9], $||\cdot||$ refers to the analogous Frobenius and two-norm for matrices and vectors respectively, while $||\mathcal{Z}||_{\mathcal{W}}$ is the W-weighted norm of $\mathcal{Z}$. The objective function in (2) is minimized by a nonlinear gradient-based optimization [10], to find the latent factor matrices $\mathbf{A}, \mathbf{B}, \mathbf{C}$.

2) Tensor Completion: This stage, reconstructs the tensor $\hat{\mathcal{Z}}$ (Recommendation tensor) from the computed factorization model $(\mathbf{A}, \mathbf{B}, \mathbf{C})$ in (2) and is given by,

$$\hat{\mathcal{Z}} = [\![\mathbf{A},\mathbf{B},\mathbf{C}]\!] = \sum_{r=1}^{R} \mathbf{a}_r \circ \mathbf{b}_r \circ \mathbf{c}_r \quad \text{or} \quad \hat{z}_{ijk} = \sum_{r=1}^{R} a_{ir}b_{jr}c_{kr}$$

where '$\circ$' refers to the outer product. Recent work [11] shows that even if a small amount of entries (CSI) are available and those are corrupted with noise, it is still possible to recover the missing entries up to the level of noise.

The recommendation tensor, $\hat{\mathcal{Z}}$ is used to obtain the recommendations, $\mathbf{z}_r(k)$ corresponding to the smoothed channel, $\mathbf{z}_p(k)$. These are the N entries of tensor $\hat{\mathcal{Z}}$ at indices corresponding to, transitions for number of scatterers, $[N_s^{k-1}, N_s^k]$ and segment number, $[S^{k-1}, S^k]$ from the last observed CSI, and the quantized levels corresponding to the smoothed channel, $\mathbf{z}_p(k)$. Let the smoothed channel for N subcarriers be, $\mathbf{z}_p(k) = [z_p(k,1), z_p(k,2) \ldots z_p(k,N)]^T$. Hence, at each iteration N recommendations $(z_r(k,n))$ are made where,

$$z_r(k,n) = \hat{\mathcal{Z}}[(N_s^{k-1}, N_s^k), (S^{k-1}, S^k), q_n] \quad (3)$$

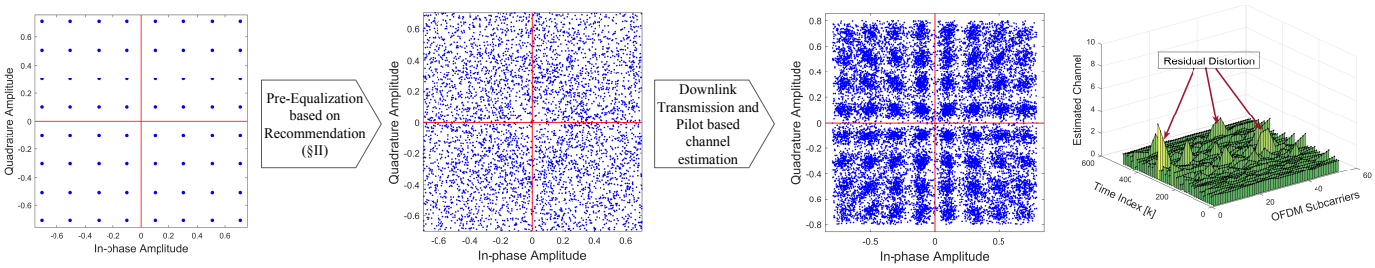

(a) Before compensation (b) After Pre-equalize (c) Received constellation (d) Equalized channel at R_x

Figure 5: High level system performance: a) The constellation ideal 64-QAM symbols used for downlink transmission. b) The ideal I/Q vectors are pre-equalized with the recommended channel profile $\tilde{\mathbf{z}}_p(k)$. c) The received symbol constellations using linear interpolation equalizer. d) The equalized channel in time and frequency domain. The estimated channel is largely flat that achieves low BER (details in §III).

for all $n = 1, \ldots, N$. Here, $\hat{\mathbf{Z}}[(N_s^{k-1}, N_s^k), (S^{k-1}, S^k), q_n)]$ is the entry of $\hat{\mathbf{Z}}$ at index $[(N_s^{k-1}, N_s^k), (S^{k-1}, S^k), q_n]$ as in figure 3 and q_n is the quantization level of $z_p(k, n)$. Then the recommended channel for N subcarriers is

$$\mathbf{z}_r(k) = \begin{bmatrix} z_r(k,1) & z_r(k,2) \ldots & z_r(k,N) \end{bmatrix}^T \tag{4}$$

The above tensor factorization method is applicable for real valued tensors. Since the actual channel is complex valued, two separate tensors are used to recommend the channel for the I/Q vectors separately.

C. Spatio-Temporal Adjustment

At each time step k, the smoothed channel $\mathbf{z}_p(k)$ is improved to $\hat{\mathbf{z}}_p(k)$ (recommended channel) by incorporating the recommendations, $\mathbf{z}_r(k)$ from (4) using a normalized weighted average:

$$\begin{aligned} \hat{\mathbf{z}}_p(k) &= (1 - \alpha_k)\mathbf{z}_p(k) + \alpha_k \mathbf{z}_r(k)) \\ &= \mathbf{z}_p(k) + \alpha_k(\mathbf{z}_r(k) - \mathbf{z}_p(k)) = \mathbf{z}_p(k) + \alpha_k \delta \mathbf{z}_p(k) \end{aligned} \tag{5}$$

where α_k is the normalization weight at time step k (a design parameter assuming a value between 0 and 1). This has the effect of updating the smoothed channel, $\mathbf{z}_p(k)$ by a delta adjustment of the form $\delta \mathbf{z}_p(k) = \mathbf{z}_r(k) - \mathbf{z}_p(k)$. A channel adjustment of this form alleviates the lag and the disparity in N_s and S. Since, the smoothed channel is adjusted with the recommendations based on the scattering environment and the location of the target vehicle, the recommended channel, $\hat{\mathbf{z}}_p(k)$ is able to account for the non-stationarity of the actual channel over time, space and vehicle density.

D. Pre-equalization at Transmitter

In order to take advantage of the recommended channel profile, the waveform of the downlink packet is pre-equalized such that when convolved with the true channel, the net effect is a flat fading at the receiver, that can be easily equalized using pilot based linear interpolation methods commonly used in V2X communication. The pre-equalized channel, $\tilde{\mathbf{z}}_p(k)$ is given by,

$$\tilde{\mathbf{z}}_p(k) = \mathbf{1}./\hat{\mathbf{z}}_p(k) \tag{6}$$

Conceptually, $\tilde{\mathbf{z}}_p(k)$ represents the inverse of the expected fading profile of the true channel, $\mathbf{z}_t(k)$ (details in §III-A). Hence, the resultant channel, $\mathbf{z}_f(k)$, as estimated by the receiver vehicle is given by Hadamard product ($\odot$, which is equivalent to convolution in time-domain),

$$\mathbf{z}_f(k) = \mathbf{z}_t(k) \odot \tilde{\mathbf{z}}_p(k) + \mathbf{w}(k) \tag{7}$$

where, $\mathbf{w}(k)$ is an additive term that captures the effect of the noise and estimation errors. The CSI, $\mathbf{z}_f(k)$, captures the interaction between the true channel $\mathbf{z}_t(k)$ and the pre-equalized channel $\tilde{\mathbf{z}}_p(k)$. At the transmitter, the measurement channel $\mathbf{z}(k)$ is computed, by combining (5) and (7),

$$\mathbf{z}(k) = \mathbf{z}_f(k) \odot \hat{\mathbf{z}}_p(k) + \mathbf{w}(k) = \mathbf{z}_f(k)./\tilde{\mathbf{z}}_p(k) + \mathbf{w}(k) \tag{8}$$

Mathematically, $\mathbf{z}(k)$ represents the error in the recommendation along with added system and numerical noise in the feedback loop. This forms the new input to the recommender system described in §II-B. Figure 5 shows the constellation diagram for a packet with 64-QAM modulation. The ideal constellation in figure 5a is pre-equalized by changing the I/Q vectors in the modulator using the recommended channel, as shown in Figure 5b. Figure 5c is the equalized constellation at the receiver with the corresponding channel profile in Figure 5d. These results show that the channel recommender system works very well for higher order constellations as well. However, there are cases when residual distortion remain at the receiver, but the penalty in BER for those cases are minimal.

III. Experiments and Results

A. Experimental setup

Figure 6 illustrates the emulated testbed to reflect a practical V2X network. The V2X channel is modeled using the WINNER channel toolbox in Matlab [12], which was used to generate 1000 channel instances for each segment (S) of the road. These channel instances are used to emulate a schedule of downlink transmissions (i.e., the true channel $\mathbf{z}_t$), by randomly selecting a segment at each time step and selecting the channel state for that segment. In reality, this schedule is not observed by the vehicles, but is used here to evaluate the accuracy and performance of the recommender system in terms of the mean square error at the transmitter and

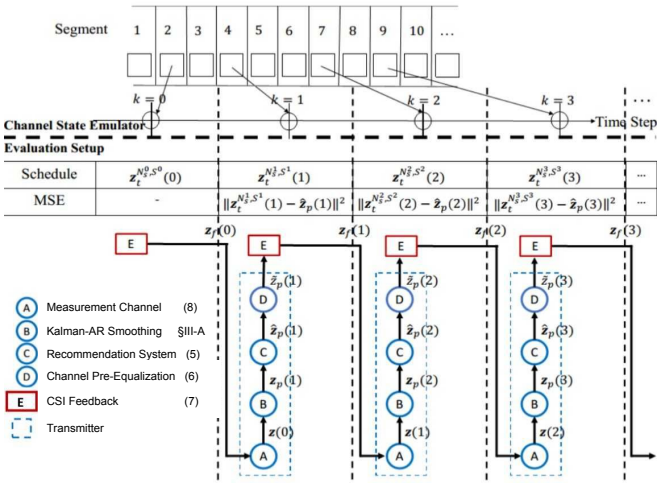

Figure 6: Measurement channel life-cycle: It shows the relationship between the true, measurement, smoothed, recommended and compensated channels (The corresponding equations are also indicated in parenthesis).

the BER and EVM at the receiver. The Winner channel toolbox has been shown to accurately reflect the real V2X channel using practical measurements in [13]. Moreover, this simulated test-bed gives the freedom to address a variety of different scenarios of the V2X channel and scattering environment that may not be observed in measurement campaigns. The parameters for the evaluation are as follows. The AR-model order is 3 (which yields the best Kalman-AR predictions), and the target vehicle's speed is $V = 20$ m/s (45 mph). The target vehicle's and the transmitter's antenna heights are 1.5m (d_{Rx}) and 2.5m (d_{Tx}) respectively, from the surface of the road. The transmitter is placed at the center of the road and it is assumed that there is a LOS propagation and the transmitter-vehicle communication link is not intercepted by large vehicles.

The number of fixed scatterers (deterministic road-side features) is assumed to be different in each segment (between 1 to 5). The number of variable scatterers is modeled as a random variable between 0 and 9. Consequently, the possible transitions, $[N_s^{k-1}, N_s^k]$, form a $(10 \times 10) \times 1 = 100 \times 1$ array. The road length is set to $d_{road} = 200$ m and divided into 20 segments (i.e. $d_{seg} = 10$ m) and the possible transitions in segment number, $[S^{k-1}, S^k]$, form a $(20 \times 20) \times 1 = 400 \times 1$ array. The number of quantization levels for the smoothed channel $\mathbf{z}_p$ (is determined by the trade-off of accuracy and computational cost of the recommender) is limited to 100, forming a 100×1 array. This data is used to construct the channel tensor $\mathcal{Z}$ of size $100 \times 400 \times 1000$. The tensor factorization rank [10] was set to $R = 2$ (which produced the least error for the recommender).

B. BER & EVM at the Receiver

Figures 7a, 7b and 7c show the BER performance. The BER corresponds to an OFDM packet of 100 random bits using different modulation and coding at a carrier frequency of $f_c = 5.9$GHz and sampling frequency of $f_s = 10$MHz. Figure 7a shows the BER performance for 16-QAM modulation and $1/2$ coding, with and without (as in conventional 802.11p) channel recommendation (with pilot-based linear interpolation equalization employed at the receiver). The frequency selective fading of V2X channel is very well compensated (shown in figure 5d) resulting in a BER improvement by almost two orders of magnitude, which is very encouraging. In contrast, conventional receiver algorithms are simply not sufficient to track the channel over space, time and frequency, hence performing much worse even at high SNR. This is another motivating reason to adopt a channel recommender at the transmitter. The ideal scenario represents an oracle with complete knowledge of channel properties, which is shown for comparison. The channel recommender requires only 7 dB more SNR to achieve the same BER ($\approx 10^{-2}$) as the ideal case as highlighted in figure 7a. Figure 7a also emphasizes the improvement in BER introduced over adaptive smoothing, by incorporating the tensor-based channel recommendations in §II-B and §II-C. Figure 7b shows the BER performance for different modulation schemes and the ability of the algorithm to support higher order modulation schemes (like 64-QAM) with very low BER. Figure 7c emphasizes the improvement in the BER performance for higher order modulations by incorporating more pilot subcarriers.

Figures 7d and 7e show the EVM performance of the channel recommender. Figure 7d shows the EVM performance for different modulation schemes, with and without channel recommendation. It shows an almost ideal performance of the EVM upto 16dB SNR, which is very encouraging. Figure 7e confirms the improvement in EVM with the number of pilots.

C. Throughput-Pilot Trade-off

In 802.11p, four pilot tones are inserted in subcarriers [-21 -7 7 21] and are used to estimate the channel. While incorporating more pilot tones, improves the channel estimation at the receiver and results in a lower BER & EVM performance and more accurate prediction of the channel (as shown in figures 7c and 7e), it reduces the theoretical throughput, since the number of active tones is less. Figure 7f shows that while the transmission throughput reduces with increasing number of pilots, the drop in the *achievable* throughput is relatively less, since the BER also decreases. Hence, we can choose higher order modulations for V2X transmission to achieve higher throughput, while maintaining the same BER. For instance, a 64-QAM scheme with 16 pilots has similar BER performance as a 16-QAM scheme with 4 pilot tones while providing higher data rate. Figure 7f also emphasizes that the recommender with a 4 pilot tone channel estimation, is sufficient to provide good BER performance and clean constellations for BPSK and QPSK and that more dense constellations require more pilots to achieve comparable BER performance due to their low margin of error (as seen in figure 5c). Using more pilots is justified for higher order modulations as they offer offer higher throughput compared to BPSK and QPSK.

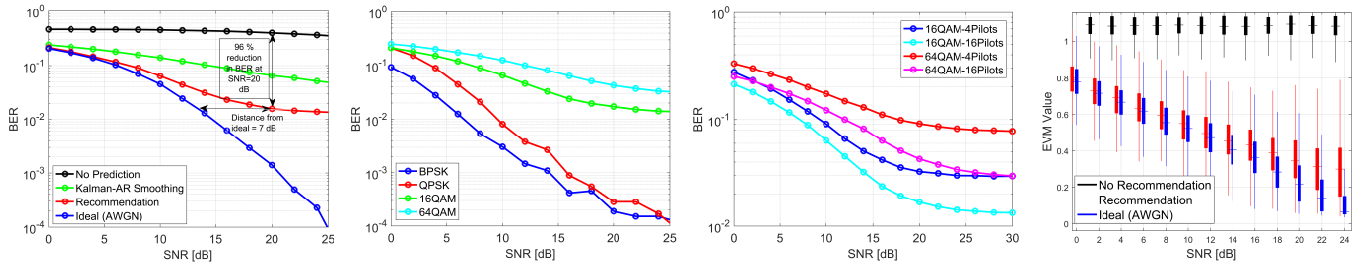

(a) BER for 16-QAM with 16 pilot tones.

(b) BER for different modulation with 16 pilot tones.

(c) BER for 16QAM and 64QAM with varying pilot tones

(d) EVM distribution for 16QAM with 16 pilot tones

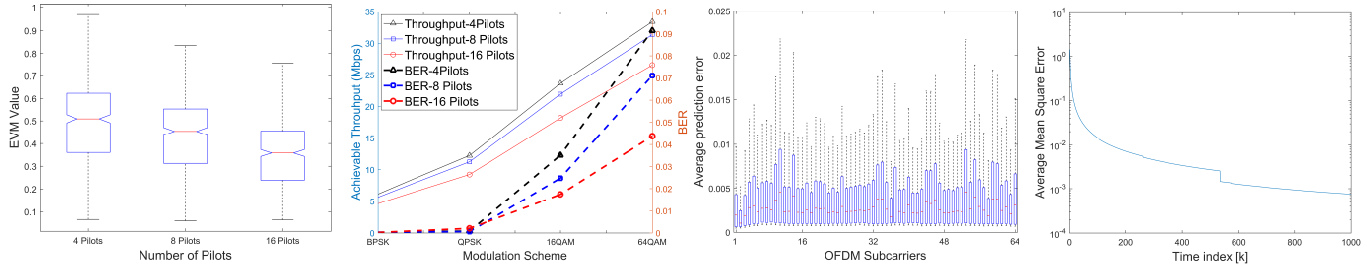

(e) EVM plot for 16QAM with varying pilot tones at 20dB SNR.

(f) Throughput and BER for different modulation for different number of pilots.

(g) Mean square error is fairly consistent for each frequency subcarrier

(h) Mean square error reduces with more CSI entries in the tensor.

Figure 7: Performance of Recommendation system at the Receiver and the accuracy of the Recommender at the Transmitter. The BER is almost *two orders of magnitude* lower than conventional methods used in 802.11p. Also, it requires only 7 dB more SNR to achieve the same BER of 10^{-2} as the ideal case (perfect estimation).

D. Accuracy of the Recommender System

Figures 7g & 7h show the accuracy of the channel recommender, in terms of the Mean Square Error (MSE) between the recommended channel coefficients and the true channel as generated in §III-A (shown in figure 6), over 1000 channel instances. Figure 7g shows that the variance about the median error and the median value of the MSE remain fairly uniform across the subcarriers, and confirms that the recommendation algorithm is able to track the non-stationary V2I channel with high accuracy. Figure 7h shows the reduction in MSE over time and the improvement in channel recommendation. It is evident that with time, as more entries are recorded, the MSE reduces since the sparsity and noise in the tensor reduces, leading to an improvement in accuracy of the channel recommender with time.

IV. Discussions

The evaluation of the V2X channel recommender system, in this work, is applicable to multiple locations for multiple vehicles. This technique is easily extensible to a complete system to address the more generic problem of V2X channel recommendations in the presence of multiple lanes, direction of traffic, varying speeds of vehicles, simultaneous multi-vehicle downlink and V2V channels. A brief sketch of the steps required in integrating the channel recommender system into a generalized real-time vehicular network is provided below and are currently being investigated using simulation and practical measurement campaigns. To address the generalized V2X channel recommendation problem the channel tensor factorization in (2) is extended to a higher-dimensional tensor $\mathcal{Z}$ (N-way tensor, for $N \geq 3$) factorization, giving way to the N-way objective function defined by,

$$f_{\mathcal{W}}(\mathbf{A}^{(1)}, \ldots, \mathbf{A}^{(N)}) = \frac{1}{2}||\mathcal{Z} - [\![\mathbf{A}^{(1)}, \ldots, \mathbf{A}^{(N)}]\!]||^2_{\mathcal{W}} + \frac{\lambda}{2}\sum_{n=1}^{N}||\mathbf{A}^{(n)}||^2 \quad (9)$$

where $[\![\mathbf{A}^{(1)}, \ldots, \mathbf{A}^{(N)}]\!] = \sum_{r=1}^{R} \mathbf{a}_r^n \circ \ldots \circ \mathbf{a}_r^n$, and the factor matrices are defined as $\mathbf{A}^{(n)} = [\mathbf{a}_1^N, \ldots, \mathbf{a}_R^N]$, with size $I_n \times R$, for $n = 1, \ldots, N$, where $\mathbf{A}^{(1)}, \ldots, \mathbf{A}^{(N)}$ are the latent factor matrices for transition in number of scatterers, segments, lanes, direction of traffic, vehicle speed etc... The objective function in (9) is minimized using the method outlined in §II-B. Tensor completion is then used to construct the recommendation tensor as, $\hat{\mathcal{Z}} = [\![\mathbf{A}^{(1)}, \ldots, \mathbf{A}^{(N)}]\!]$ and obtain the recommended channel, $\hat{\mathbf{z}}_p(k)$ similar to §II-B and §II-C. This shows the adaptability of the recommender approach to address a variety of V2X scenarios.

V. Related Work

V2X channels are inherently non-stationary and are particularly difficult to analyze [14]. Decision Feedback Equalization (DFE) has been adopted in [15] at the cost of complex feedback paths, which we eliminate by employing a channel recommender at the transmitter to pre-equalize the channel. Fast varying vehicular environments are addressed in [16] using the extended Kalman filter, but is restricted to a deterministic evolution of the channel. Approaches that used the Kalman filter to track the non-stationarity statistics of a time series [6],

[7], do not adapt well for spatio-temporal channel equalization and for higher order modulation techniques (details in §II).

Latent factor recommenders enable the extraction of recommendations when the underlying system-process is unknown [17]. Tensor factorization based recommenders have been adopted for multi-channel EEG analysis for sparse and noisy data in [18]. Tensor completion has been employed to recover missing entries of a tensor in the context of Network traffic data in [10]. Temporal tensor models for recommendation, designed to learn time-evolving patterns (such as periodicity) in data [19] and where time is considered as a separate dimension in the tensor [20], are impractical for V2X channels due to their inherent non-stationarity and are not scalable over time. The space-time-frequency tensor-recommender for EEG data in [18], also suffers from the same temporal scalability issues. In contrast, we design a spatio-temporal recommender, with a Kalman-AR smoother to address the time evolution of the V2X channel statistics, enabling the design of the channel tensor without a separate time dimension, to address the non-stationarity over space and time. Thus, limiting the size of the channel tensor database and consequently, causing the recommendations to improve over time.

In the context of vehicular networks and wireless communications, recommender systems have been adopted in vehicular social networks [21], network traffic data [10], wireless channel selection [22] and abundantly in the context of IoT [23]. However, to the best of our knowledge have not been employed for channel equalization in wireless and V2X communications. This emphasizes the challenging nature of the problem and the novelty of this work.

VI. Conclusion

In this work, we have shown the power of recommender systems when applied to highly dynamic wireless environments like V2X networks. Through modelling, analysis and simulations, we draw three conclusions: 1) The channel recommender is able to successfully predict the V2X channel to obtain 96% lower BER in spatio-temporal, non-stationary channels by resulting in an almost flat fading profile at the receiver, 2) This enables higher modulation schemes to be used in V2X communications for high throughput, and 3) The accuracy of the recommender system improves with time and asymptotically achieving an MSE of 10^{-3}. Therefore, the encouraging results from this work will form the core of robust and highly reliable V2X networks supporting demanding mobile applications.

References

[1] US Department of Transportation, "Intelligent transportation system joint program office." [Online]. Available: http://www.its.dot.gov

[2] M. Boban, T. T. V. Vinhoza, M. Ferreira, J. Barros, and O. K. Tonguz, "Impact of vehicles as obstacles in Vehicular Ad Hoc Networks," *IEEE Journal on Selected Areas in Communications*, vol. 29, no. 1, pp. 15–28.

[3] M. Boban, J. Barros, and O. K. Tonguz, "Geometry-Based Vehicle-to-Vehicle Channel Modeling for Large-Scale Simulation," vol. 63, no. 9, pp. 4146–4164, 2014.

[4] T. Svensson, M. Werner, R. Legouable, T. Frank, and E. Costa, "WINNER II Channel Models," vol. 1, no. 206, pp. 1–206, 2007. [Online]. Available: http://projects.celtic-initiative.org/WINNER+/WINNER2-Deliverables/D4.6.1.pdf

[5] IEEE Computer Society : LAN/MAN Standards Committee, *Part 11: Wireless LAN Medium Access Control (MAC) and Physical Layer (PHY) Specifications, Amendment 6: Wireless Access in Vehicular Environments (WAVE)*, 2010.

[6] M. Arnold, W. H. R. Miltner, H. Witte, R. Bauer, and C. Braun, "Adaptive AR modeling of nonstationary time series by means of Kalman filtering," *IEEE Trans. Biomed. Eng.*, vol. 45, no. 5, pp. 545–552, 1998.

[7] M. Al-Ibadi and A. Dutta, "Predictive analytics for non-stationary v2i channel," in *2017 9th International Conference on Communication Systems and Networks (COMSNETS)*, Jan 2017, pp. 243–250.

[8] X. Wu, S. Subramanian, R. Guha, R. G. White, J. Li, K. W. Lu, A. Bucceri, and T. Zhang, "Vehicular communications using dsrc: Challenges, enhancements, and evolution," *IEEE Journal on Selected Areas in Communications*, vol. 31, no. 9, pp. 399–408, September 2013.

[9] T. G. Kolda and B. W. Bader, "Tensor decompositions and applications," *SIAM Review*, vol. 51, no. 3, pp. 455–500, 2009. [Online]. Available: https://doi.org/10.1137/07070111X

[10] E. Acar, D. M. Dunlavy, T. G. Kolda, and M. Mørup, "Scalable tensor factorizations for incomplete data," *Chemometrics and Intelligent Laboratory Systems*, vol. 106, no. 1, pp. 41 – 56, 2011, multiway and Multiset Data Analysis. [Online]. Available: http://www.sciencedirect.com/science/article/pii/S0169743910001437

[11] E. J. Candès and T. Tao, "The power of convex relaxation: Near-optimal matrix completion," *CoRR*, vol. abs/0903.1476, 2009. [Online]. Available: http://arxiv.org/abs/0903.1476

[12] M. C. S. T. Team, "Winner ii channel model for communications system toolbox," Available online, October 2016. [Online]. Available: https://www.mathworks.com/matlabcentral/fileexchange/59690-winner-ii-channel-model-for-communications-system-toolbox

[13] S. Jaeckel, L. Raschkowski, K. Börner, and L. Thiele, "Quadriga: A 3-d multi-cell channel model with time evolution for enabling virtual field trials," *IEEE Transactions on Antennas and Propagation*, vol. 62, no. 6, pp. 3242–3256, June 2014.

[14] C. F. Mecklenbraüker, A. F. Molisch, J. Karedal, F. Tufvesson, A. Paier, L. Bernadó, T. Zemen, O. Klemp, and N. Czink, "Vehicular channel characterization and its implications for wireless system design and performance," *Proceedings of the IEEE*, vol. 99, no. 7, pp. 1189–1212, 2011.

[15] K. Sil, M. Agarwal, D. Guo, M. L. Honig, and W. Santipach, "Performance of turbo decision-feedback detection for downlink OFDM," *IEEE Wireless Communications and Networking Conference, WCNC*, pp. 1488–1492, 2007.

[16] E. P. Simon, H. Hijazi, L. Ros, M. Berbineau, and P. Degauque, "Joint estimation of carrier frequency offset and channel complex gains for ofdm systems in fast time-varying vehicular environments," in *2010 IEEE International Conference on Communications Workshops*, May 2010, pp. 1–5.

[17] Y. Koren, "1 the bellkor solution to the netflix grand prize," 2009.

[18] F. Miwakeichi, E. Martínez-montes, B. P. A. Valdés-sosa, N. Nishiyama, A. H. Mizuhara, and Y. Y. A, "Decomposing eeg data into space-time-frequency components using parallel factor analysis," *Neuroimage*, p. 2004.

[19] E. Frolov and I. V. Oseledets, "Tensor methods and recommender systems," *CoRR*, vol. abs/1603.06038, 2016. [Online]. Available: http://arxiv.org/abs/1603.06038

[20] D. M. Dunlavy, T. G. Kolda, and E. Acar, "Temporal link prediction using matrix and tensor factorizations," *ACM Trans. Knowl. Discov. Data*, vol. 5, no. 2, pp. 10:1–10:27, Feb. 2011. [Online]. Available: http://doi.acm.org/10.1145/1921632.1921636

[21] T. Li, M. Zhao, A. Liu, and C. Huang, "On selecting vehicles as recommenders for vehicular social networks," *IEEE Access*, vol. 5, pp. 5539–5555, 2017.

[22] H. Sun, Y. Zhong, and W. Zhang, "Channel selection through a recommender system," in *2010 International Conference on Wireless Communications Signal Processing (WCSP)*, Oct 2010, pp. 1–5.

[23] I. Mashal, O. Alsaryrah, and T. Y. Chung, "Analysis of recommendation algorithms for internet of things," in *2016 IEEE Wireless Communications and Networking Conference Workshops (WCNCW)*, April 2016, pp. 181–186.